Paper No. T3-1.3, pp. 1-5

15th INTERNATIONAL SYMPOSIUM on POWER ELECTRONICS - Ee 2009
XV Međunarodni simpozijum Energetska elektronika – Ee 2009
NOVI SAD, REPUBLIC OF SERBIA, October 28th - 30th, 2009

P-SPICE MODELING OF AN INDUCTION COIL - HEATED PIECE SYSTEM IN AN INDUCTION HEATING SOLID-STATE INSTALLATION

Dobroslav Dankov
University of Gabrovo, Departament of Electronics,
Gabrovo, Bulgaria, dankov@tugab.bg

Abstract: *The present paper views modeling and computer simulation process of a high-frequency solid-state induction heating installation. An appropriate model for the induction coil - heated piece system is proposed and a P-SPICE simulation of the induction coil operation has been realized. The theoretical mathematical model and the simulation model have been compared and the obtained results have been experimentally verified.*

Key Words: ***Induction Heating, Induction Coil, Class-DE Inverter, IGBT, P-SPICE***

1. INTRODUCTION

Computer simulation of the operation of power electronic devices has become increasingly common recently, since it often complements the design and mathematical modeling of electromagnetic processes in power electronic devices [1-3].

Determining precisely the currents and voltages, static and dynamic losses in power switches and backward diodes is essential with view to determining the dissipated power of each element and the correct choice of the most efficient cooling method. In this way the efficiency of the installation is improved and the production costs are reduced. Moreover, the design of power electronic devices is facilitated, in particular electronic-technological induction heating /IH/ installations.

A definite problem with these installations is explaining the equivalent parameters of the load and their variation during the heating process, since they have a direct influence on electromagnetic processes in solid-state inverters used as high-frequency power supplies in IH installations.

The PURPOSE of the present paper is to propose a suitable equivalent circuit of the induction coil-workpiece system in order to improve the accuracy in P-SPICE simulation of the operation of a real transistorized induction heating installation.

2. DEVELOPMENT

In IH applications the load is the induction coil - heated metal piece system. This piece is located inside the induction coil and parallel to the coil that induces a magnetic field.

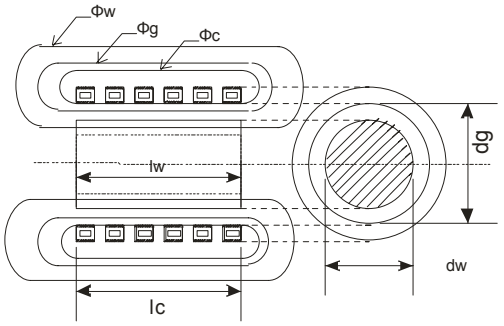

Fig.1. *Induction coil - workpiece system in IH.*

The piece and the induction coil are magnetically connected through the magnetic field, the same way as in a transformer – Fig.1. The induction coil, which is supplied by the power supply source, is the transformer primary, while the metal being heated is the secondary, which has one shorted turn [5].

Having in mind the transformer operation principle, the equivalent circuit is shown in Fig.2 (a).

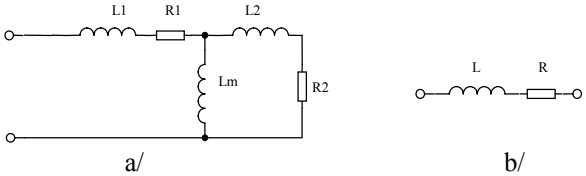

Fig.2. *Equivalent circuits of the load in IH.*

Very often this equivalent circuit is too complex to be applied. Normally the equivalent circuit presented in Fig.2 (b) is used. From this circuit the characteristics of the resonant load can be obtained in terms of the quality factor and the resonance frequency, which are most commonly used for designing the induction heating systems. Comparing Fig.2 (a) to Fig.2 (b), it can be

noticed that the inductance (dissipation inductance) has been ignored in the second circuit. In addition, the parameters of the equivalent circuit are a function of the operating frequency. When the frequency rises, the value of the equivalent resistance also rises, while the value of the equivalent inductance falls due to the skin effect. This particularity makes the analysis more difficult, especially when the current through the load contains too many harmonics. In order to determine the parameters of the induction coil equivalent circuit or to design an induction coil from the known parameters, the relation between the equivalent and the real parameters of the induction heated piece has to be found.

The magnetic flux of the induction coil has three components: ϕ_w – magnetic flux that closes across the piece; ϕ_g – magnetic flux across the air gap; ϕ_c – magnetic flux across the surface of the induction coil [6].

$$\varphi_w = \int_0^R 2\pi r \mu H dr = 2\pi\mu H_s \tag{1}$$

It can be rationalized to

$$\varphi_w = \mu H_s A_w (q - jp) \tag{2}$$

where $A_W\ (m^2)$ – the piece cross-section. The air gap in the induction coil is usually large due to the need for thermal insulation and the necessity for mobility of the piece, hence the magnetic flux in the gap is considerable.

$$\varphi_g = \mu_0 H_s A_g \tag{3}$$

where $A_g\ (m^2)$ – the cross-section of the air gap area.

The precise calculation of the flux across the induction coil surface is a complex task. We assume that the induction coil can be presented as a tube whose diameter is greater than the skin depth.

$$\varphi_c = k_r \frac{\mu_0 \delta_c \pi d_g}{2} H_s (1 - j) \tag{4}$$

where k_r is a correlation coefficient and depends on the magnetic flux between the induction coil turns, and δ_c – skin depth of the induction coil. The total magnetic flux is:

$$\varphi_0 = \varphi_w + \varphi_g + \varphi_c$$

$$\varphi_0 = \mu_0 H_s \left[\begin{array}{l} \left(A_g + \mu_r q A_w + k_r \dfrac{\delta_c \pi d_g}{2} \right) - \\ j \left(\mu_r p A_w + k_r \dfrac{\delta_c \pi d_g}{2} \right) \end{array} \right] \tag{5}$$

Assuming that the induction coil is relatively long, or there ϕ_0 is a ferromagnetic external circuit (there is no magnetic resistance in the induction coil outer area), the total magnetic force is used for the magnetic field, and the magnetic field strength across the surface becomes:

$$H_s = \frac{I_c N_c}{l_c} \tag{6}$$

where Nc – number of induction coil turns, Ic – current across the induction coil, lc – induction coil length.

The effective value of the voltage across the induction coil is:

$$u_{ind} = N_c \frac{d\varphi_0}{dt} = j 2\pi f N_c \varphi_0 \tag{7}$$

Hence, after the substitution, we obtain

$$u_{ind} = \frac{2\pi f \mu_0 N_c^2}{l_c} I_c \left[\begin{array}{l} \left(\mu_r p A_w + k_r \dfrac{\delta_c \pi d_g}{2} \right) + \\ j \left(A_g + \mu_r q A_w + k_r \dfrac{\delta_c \pi d_g}{2} \right) \end{array} \right] \tag{8}$$

This is an equation to determine the voltage drop across the five elements connected in series. Following these equations, Fig. 2 (a) is transformed into Fig.3.

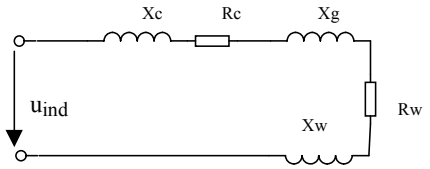

Fig.3. *Transformed equivalent circuits of the load in IH.*

R_W is the equivalent resistance of the workpiece and it is proportional to parameter *p* – Fig.4.

$$R_w = \frac{2\pi f \mu_0 N_c^2}{l_c} \mu_r p A_w \tag{9}$$

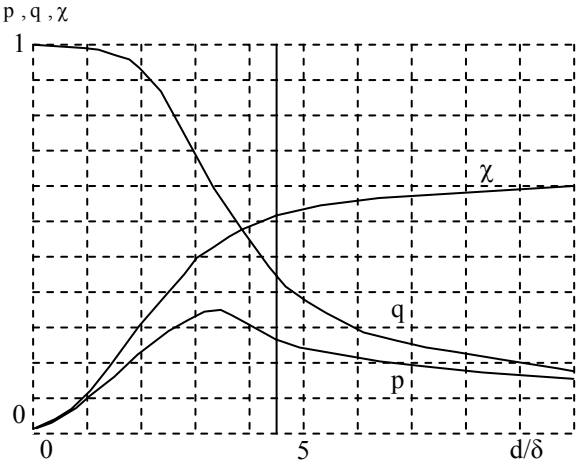

Fig.4 *Dependence of the active p and the reactive q power components, as well as the power factor χ on the ratio between the piece diameter* ***d*** *and the skin depth* δ_w *for a cylindrical piece.*

R_C is the equivalent resistance of the inductor. X_W is the equivalent inductive reactance of the workpiece and it is proportional to parameter *q*. X_g is the inductive reactance of the air gap. X_C is the internal inductive reactance of the inductor.

$$R_c = \frac{2\pi f \mu_0 N_c^2}{l_c} k_r \frac{\delta_c \pi d_g}{2} \tag{10}$$

$$X_w = j \frac{2\pi f \mu_0 N_c^2}{l_c} \mu_r q A_w \tag{11}$$

$$X_g = j \frac{2\pi f \mu_0 N_c^2}{l_c} A_g \tag{12}$$

$$X_c = j \frac{2\pi f \mu_0 N_c^2}{l_c} k_r \frac{\delta_c \pi d_g}{2} \tag{13}$$

The inductor efficiency is obtained from:

$$\eta = \frac{R_w}{R_w + R_c} \qquad (14)$$

The inductor power factor is:

$$\cos\varphi = \frac{R_w + R_c}{Z} \qquad (15)$$

where $Z = \sqrt{(R_w + R_c)^2 + (X_w + X_g + X_c)^2}$ (16)

It can be seen that the equivalent parameters of the inductor - piece system depend both on the geometrical dimensions, and on the magnetic permeability μ_0 and the internal resistance ρ of the piece being heated, which are largely dependent on temperature [5]. In order to create a suitable model for P-SPICE, these dependences should be presented by the analytical expressions:

$$\mu_r = 1 + \frac{\alpha . H_s^{\beta} - 1}{(1 + (\frac{T}{T_k - T})^{\chi})^{\delta}} \qquad (17)$$

where $\alpha=3.10^5$, $\beta=-0,85$, $\chi=1,9$, $\delta=0,16$.

For temperatures above Curie temperature – $T_к$, the magnetic permeability of carbon steels becomes $\mu=1$. The workpiece internal resistance depends on the metal temperature coefficient α_T and is obtained from the relationship:

$$\rho(T) = \rho_0 . (1 + \alpha_T . T) \qquad (18)$$

The simulation begins with the inductor equivalent parameters for the first workpiece having a diameter D=30mm for cold metal. The results for the equivalent elements of the inductor-workpiece system have been obtained as a result of calculations according to formulae (9)-(16) and the equivalent circuit in Fig.3.

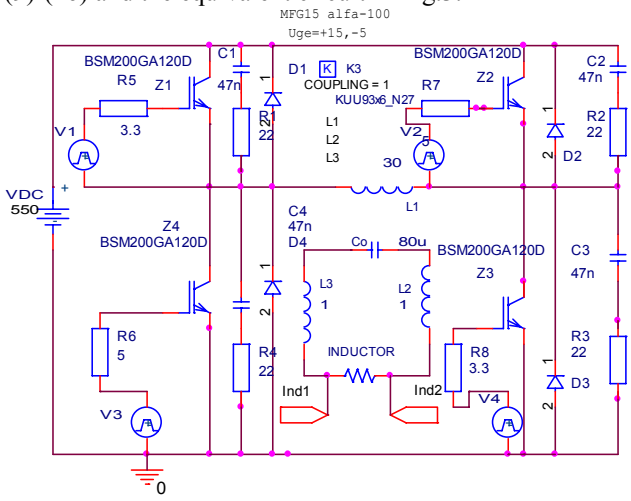

Fig.5 a. *Circuit of IGBT transistorized inverter of the induction heating installation.*

As a result of the proposed model we can study the inverter more thoroughly as regards the effect of temperature change, air gap size, number of inductor turns, as well as the geometrical dimensions of the inductor - workpiece system. All these manufacturing parameters have a direct influence on the electromagnetic processes in the inverter, modifying the operating point of the transistors, the current and voltage values in the A.C. part of the inverter and the development of the commutation processes.

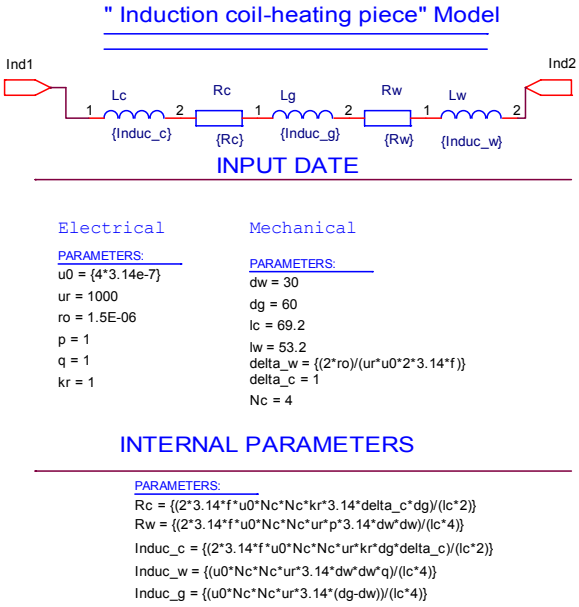

*Fig.*5 b. *Model of the inductor - workpiece system for computer simulation using P-SPICE.*

Fig.6-9 shows the effect of some of these parameters on the change in current in the inverter diagonal (the sum of the two currents through the individual transistors in the inverter diagonals), the output voltage across the load and the commutation processes in the transistors. Table 1 presents generalized data about the values of the elements, the initial values for the different ranges, and the average values of the current through the transistors and the backword diodes and the voltage across the circular capacitor as a result of the simulation for cold and hot metal.

Table 1. *Simulation results.*

For cold metal – **d=30mm:**								
Pout, kW	**∠ λ, °**	**Iin, A**	**f0,kHz**	**I_{VT}, A**	**I_{VD}, A**	**t_{VR}, μS**	**Ioff, A**	**U_1, V**
35	171	77	14,6	122	1.32	2.5	84.82	154
For hot metal (above Curie temperature)- **d=30mm:**								
Pout, kW	**∠ λ, °**	**Iin, A**	**f0,kHz**	**I_{VT}, A**	**I_{VD}, A**	**t_{VR}, μS**	**Ioff, A**	**U_1, V**
40	171	92	17.8	191	5.24	2.5	97.2	272

Fig.6-9 shows time-charts of the simulation for operation with 2 different conduction angles, i.e. in case of regulation, for a minimum and a maximum output power.

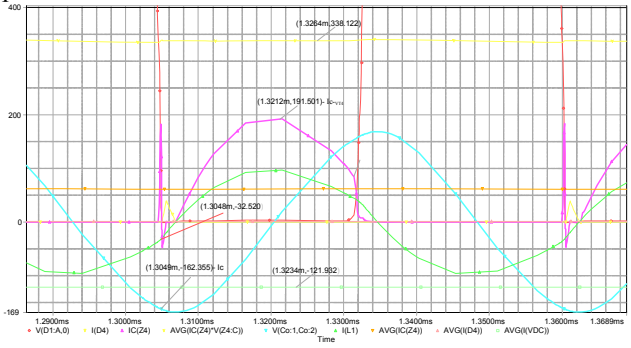

Fig.6. *P-SPICE time-charts for UDS, ID of VT4 and the voltage across the circular capacitor Uc in a bridge*

class-DE quasi-resonant inverter for λ≈171° and hot metal.

Error! Objects cannot be created from editing field codes. Fig.7. *P-SPICE time-charts for U_{DS}, I_D and loss power Рзаг. of VT4 in bridge class-DE quasi-resonant inverter for λ≈171°.*

Fig.7 shows the turning-off of the transistors for almost zero voltage in series class-DE quasi-resonant IGBT inverter for induction heating, i.e. there is a ZVS „soft" commutation.

It can be seen that the condition for ZVS commutation is observed – the inductor operates with inductive detuning, the value of the resonance commutation capacitor being correctly chosen for the different turn-off currents

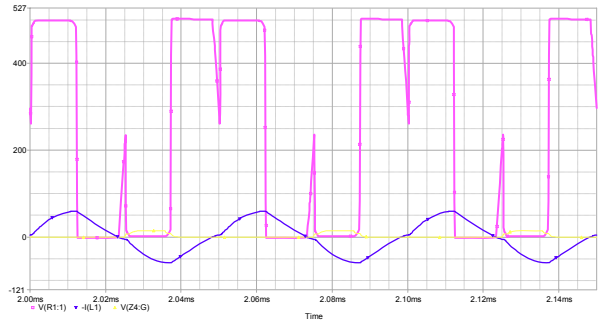

Fig.8. *P-SPICE time-charts for U_{DS}, I_D of VT4 in a bridge class-DE quasi-resonant inverter for λ≈80°.*

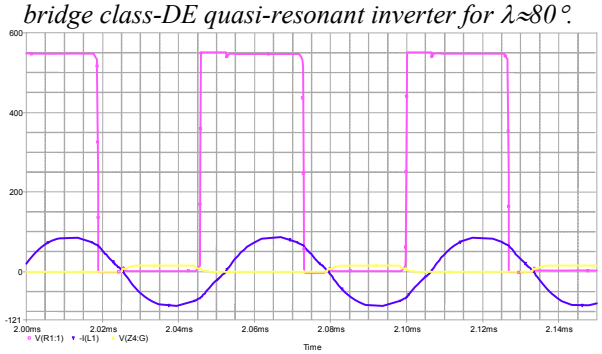

Fig.9. *P-SPICE time-charts for U_{DS}, I_D of VT4 in a bridge class-DE quasi-resonant inverter for λ≈170°.*

The inverter is operational over a wide range of power regulation, without any effect on the transistors' commutation manner.

To verify the results obtained from the computer simulation, an induction installation for volumetric heating of metals of maximum active output power 40 kW is used.

The experimental set-up for heating the above-mentioned piece by the induction installation with the bridge class-DE IGBT quasi-resonant inverter is shown in Fig.10.

Fig.10. *Practical realization.*

Table 2. *Experimental results*

Conduction angle -∠ λ, °	171	125	107	78
Frequency - f, kHz	17	18.5	19	20.8
Master pulse width - tu, μS	28	18,8	15,67	10,5
Max. current through IGBT - Imax, A	130	96	81	65
Mean value of input current - Iin, A	90,9	54,5	36,4	18,2
Output power - Pout, kW	40	22	11,9	4,77

Table 2 presents systematized values in series class-DE quasi-resonant IGBT inverter for IH as a result of the experimental measurements for cold metal.

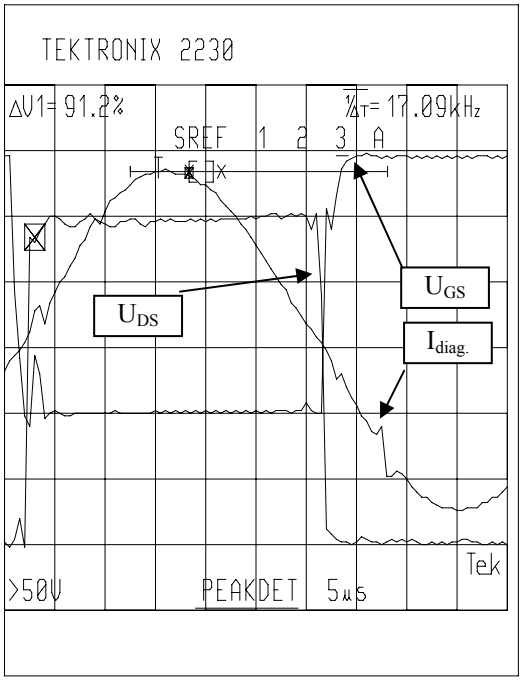

Fig.11. *Oscillograms for U_{GS} (div=5V), U_{DS} (div=100V), U_{GS}(div=5V) of VT04 and $I_{DIAGONAL}$ (div=100A) for and P_{out}=40 kW (α≈171).*

Fig.11 presents the experimental data from the operation of the 50 kW/30kHz bridge IGBT inverter for IH with output power regulation.

In comparison with the experimental values, the simulation exhibits some deviations, which can be accounted for by inaccuracies in modeling, however the error does not exceed 20%.

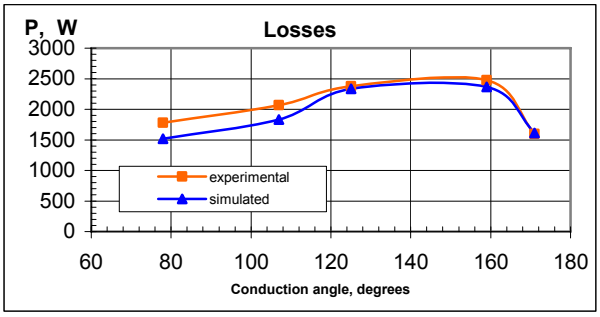

Fig.12. *Simulated and experimentally measured losses in the converter.*

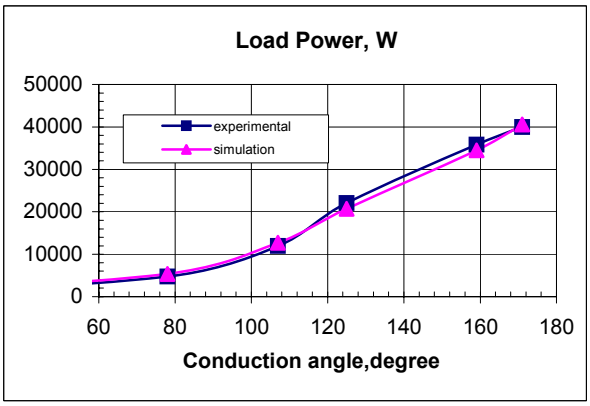

Fig.13. *Regulating characteristic of the inverter.*

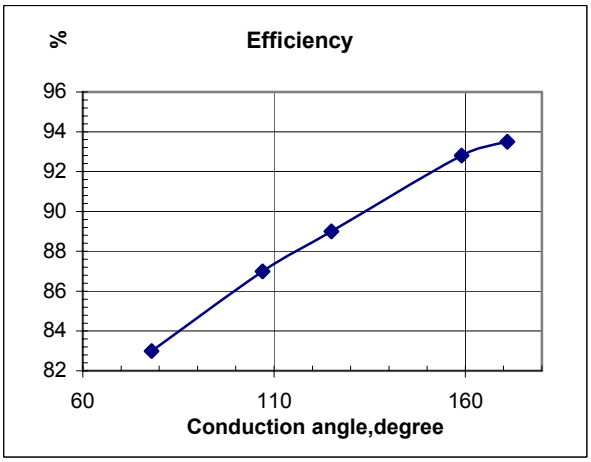

Fig.14. *Graph of efficiency change during regulation.*

Fig.12 compares graphically the simulated and the experimentally measured losses in the converter, the losses in the inverter transistors being added to the losses in the rectifier unit.

The obtained data have been used as a basis for constructing the regulating characteristic of the inverter – Fig.13. Fig.14 presents a graph illustrating the change in the inverter efficiency as a function of the regulation angle.

3. CONCLUSION

The proposed model of the induction coil - piece system for induction heating can be used successfully for simulation of the inverter operation in an induction heating installation. Moreover, there is no need for preliminary calculation of the system equivalent elements, it is sufficient to input the mechanical dimensions and the electrical parameters of the metal piece to be heated.

This would help for the correct dimensioning of the inverter, and also for observing the interaction of the inverter with the induction coil - piece system over the entire range of the piece temperature variations.

The proposed model analytically records the change in metal parameters in the course of heating – μ and ρ, and hence follows a further development of the model presented in [4]. The improvement of the model along this line increases the benefit derived from the simulation of the electromagnetic processes in the inverter, also covering the dynamics during heating. This would help for the correct dimensioning of the inverter, as well as for observing the interaction of the inverter with the inductor - workpiece system over the entire range of the piece temperature variations.

5. REFERENCES

[1] Blinov Yu., Kashanov B., Ishin V., Brawn E.: "*Numerical Simulation of Solid State Power Supplies for Induction Heat and Feeding Network*", International Induction Heating Seminar – 98, pp.17-25.

[2] Chindris M., Stefanescu S., Sudria A., Vadan I., "*Series-Resonant Inverter Structure Suitable for Induction Heating Applications*", International Induction Heating Seminar – 98, pp.47-55.

[3] Moham N., Undeland T. M., Robbins W. P., "*Power Electronics, Converters, Applications and Design*". New York: Wiley, 2005.

[4] Simeonov M., Dankov D., Tzonev E. "*ZVS Class-DE Full-Bridge Resonant Inverter for Induction Heating*". 12th International Symposium on Power Electronics - Ee 2003 CD, Paper No. T1-1.2, pp. 1-5.

[5] Sluhotskij A.E. "*Induction Heating Instalations*". St.Petersburg, Energoizdat, 1981.(in Russian).

[6] Ying J., "*Resonant and Quasi-resonant inverters for Hight-frequency induction heating*", Desertation, Berlin, 1995.